Science in China Series D: Earth Sciences

Magnetic properties of sediments from the Pearl River Delta, South China: Paleoenvironmental implications

YANG XiaoQiang[1†], Rodney GRAPES[1], ZHOU HouYun[2] & YANG Jie[1]

[1] Department of Earth Sciences, Sun Yat-Sen University, Guangzhou 510275, China;
[2] Guangzhou Institute of Geochemistry, Chinese Academy of Sciences, Guangzhou 510640, China

Magnetic parameters and their environmental implications of sediments in a core (PD) from the Pearl River Delta, South China, indicate that ferrimagnetic minerals with low coercivity, such as magnetite, dominate the magnetic properties although small amounts of Fe-sulphides occur. The fraction of Fe-sulphides increases and becomes the dominant minerals determining the magnetic characteristics in grey-black organic-rich clay horizons, indicating an anoxic, sulphate-reducing swamp environment resulting from a marine regression. In the "Huaban clay", hard magnetic minerals, such as hematite and goethite, largely control the magnetic properties of the sediments and imply a long period of exposure and weathering. Where magnetite is the main magnetic mineral, its fraction and grain size determine properties such as magnetic susceptibility (κ) and saturation isothermal remanent magnetization (SIRM). Ratios of SIRM/κ and χ_{arm}/SIRM reflect changes in sea level with high SIRM/κ and χ_{arm}/SIRM correlating with a smaller magnetic mineral grain size and rising sea level. Based on downcore variations of these environmental magnetic parameters along with sediment characteristics and microfauna, the sedimentary environment of the Pearl River Delta area can be divided into two main cycles of transgression and regression during the late Pleistocene and Holocene with more sub-cycles of sea level fluctuation during each transgression.

the Pearl River Delta, rock magnetic properties, environmental magnetic signatures, sedimentary environment, sea-level change

1 Introduction

Deltaic sediments provide good information on the interaction between marine and fluvial systems and climatic change. Although studies in climatology, stratigraphy and geochemistry have provided considerable information on high-frequency sea-level fluctuations and global climate change[1−5], some key issues such as establishment of a reliable chronology are still not thoroughly addressed due to the complexity of sedimentation dynamics, transverse face changes and erosion during marine regression. In the past decades, the successful application of the environmental magnetic method in ellucidating climatic change and comparing marine and lacustrine sediment records with the Chinese loess-paleosols sequence[6−9] suggests that this method may be useful in the study of deltaic sediments. To test this, it is necessary to understand the magnetic properties of deltaic sediments, and the basic parameters of the magnetic minerals, such as their characterisation, sources, grain size and concentration. In this paper, sediments from the Pearl River Delta, southern China, are used to investigate details of their magnetic characteristics in relation to environmental changes during the formation of the Pearl River Delta.

Received April 21, 2007; accepted August 31, 2007
doi: 10.1007/s11430-007-0151-4
†Corresponding author (email: eesyxq@mail.sysu.edu.cn)
Supported by the National Natural Science Foundation of China (Grant Nos. 40104002, 40674034 and 40331009), and the Natural Science Foundation of Guangdong Province, China (Grant No. 06023110)

2 Geographic setting and core description

The Pearl River system comprises the Xijiang, Beijiang and Dongjiang rivers and is the third largest river in China. The Pearl River Delta is a zone of > 10000 km^2 in southern Guangdong Province, South China (Figure 1), and is surrounded by low mountains and hills mainly of granite. The delta began to develop since the late Pleistocene, receiving sediments consisted mainly of clay, silty clay and fine sand. Its thickness varies with the fundus from several meters to several decameters. Sedimentation rates change between 50—200 cm/ka in different areas[10,11].

Core PD is located in Guangzhou city at 22°53.676′N, 113°28.589′E, about 50 km off estuary. It was obtained by the method of circumvolving coring using a plastic tube driven into the sediments. The core is 17.5 m in length, and from bottom to top, comprises the following sequences: grey coarse sand with fine gravel (17.5—15.2 m), grey silt and fine sand (15.2—13.9 m) and grey, grey-black clay, silty clay and clayey sand with foraminifera, ostracods and other microfauna found between 13.9—0 m. At the intervals of 12.02—11.99 m, 10.39—10.30 m and 9.13—7.4 m multicoloured (yellow, red, white, grey, etc.) clay horizons occur that are commonly referred to as the "Huaban clay".

3 Sampling and analytical methods

After the core was split lengthwise, U-channel samples were collected by pushing rigid U-shaped plastic liners, 2×2 cm in cross-section and up to 100 cm in length, into the halved PD core analyses of volume susceptibility, isothermal remanent magnetization (IRM) and anhysteretic remanent magnetization (ARM) measurements. About 0.6 g of powdered sediment was prepared for χ-T measurement, and 12 discrete cubic samples (1.9 cm×1.9 cm×1.9 cm) were obtained for saturation remanent magnetization (SIRM), coercivities of remanence (H_{cr}) and thermal demagnetization on three axes.

Magnetic measurements were conducted on a 2G-760 system at 2 cm intervals. First, volume susceptibility was acquired, then anhysteretic remanent magnetization (ARM) measurement was made in an 80 mT AF and a 0.05 mT biasing field. Isothermal remanent magnetization (IRM) was acquired in fields of 100 mT, 1 T and –300 mT. SIRM in steps up to a maximum field of 2.7 T and H_{cr} were carried out on the discrete cube samples using a 2G-660 pulse magnetizer and JR-5A. Parallel-samples were magnetized on the *x*, *y*, *z* axes at 2.7 T, 0.5 T and 0.05 T respectively, followed by thermal demagnetization between 0—700℃ in a TSD-1 furnace with remanence measured on a JR-5A at every temperature point. The temperature dependence of magnetic susceptibility was measured using a KLY-3S kap-

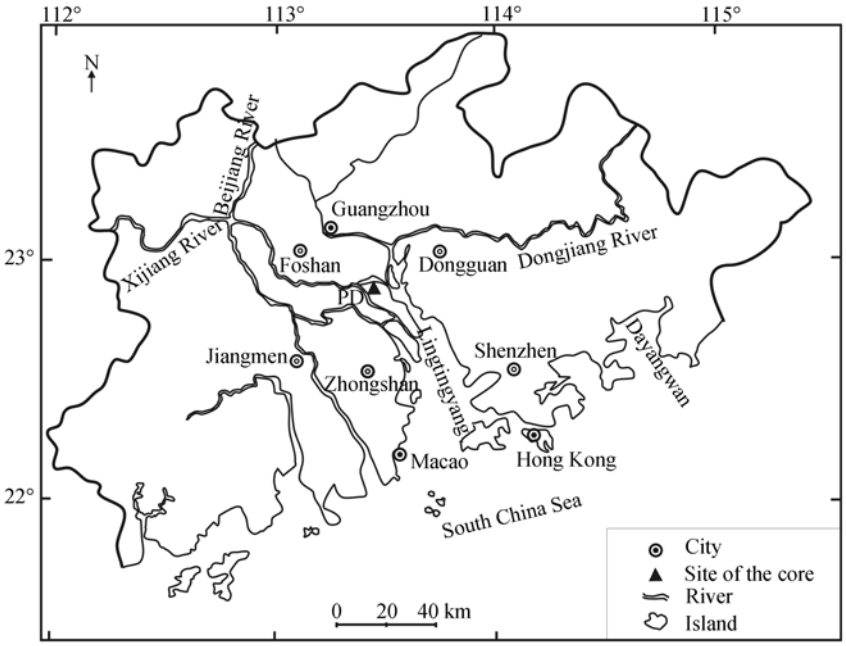

Figure 1 Location of the Pearl River Delta and PD core.

pabridge with a CS-3 high-temperature device in an argon atmosphere in a heating-cooling cycle from room temperature to 700℃ and back to room temperature. Hysteresis loops were measured in fields of up to maximum of 1 T using a Micromag 2900. All magnetic experiments were conducted at the Paleomagnetism and Geochronology Laboratory of the Institute of Geology and Geophysics, Beijing, CAS and the Paleomagnetism Laboratory of China University of Geosciences, Beijing.

Magnetic particles were extracted from the sediments at selected depths for X-ray diffraction (XRD) (D/Max -IIIA) and energy dispersive X-ray (EDS) (ISIS-300) analyses at the Instrumental Analysis & Research Center of Sun Yat-Sen University, Guangzhou. Colour measurement of the sediments was carried out in the Laboratory of Cenozoic Geology and Environment, Institute of Geology and Geophysics, CAS, Beijing.

4 Results

4.1 X-ray powder diffraction and energy dispersive analysis

The magnetic mineral assemblage of the core sediments can be divided into three types based on X-ray powder diffraction patterns and energy dispersive analysis of 14 samples from different depths of the core representing different sediments. In shallow greyish-black or grey silty clay, clayey silt and grey silt, and fine sand (first type), titanomagnetite and Fe sulphides are present (Figure 3(a)). In the dark grey-black compact clay at intervals of 0—44 cm (top) and 913—1010 cm (middle) (second type), pyrite, pyrrhotite and a Fe-Ti oxide are the dominant magnetic minerals (Figures 2(c) and 3(b)). In the "Huaban clay" horizons (third type) distributed in the middle of the core (at depth between 913—740 cm), the main magnetic minerals are greigite and some Fe-Ti oxides (Figure 3(c)).

4.2 High temperature susceptibility measurements

Heating curves for sediments of the first type do not show significant variation over a temperature range from room temperature to ~280℃ but show rapidly increasing susceptibility at 280℃ or 350℃, reach a maximum at 450℃ or 510℃ followed by decreasing susceptibility with a further increase in temperature. Magnetite and hematite are indicated by a pronounced decrease

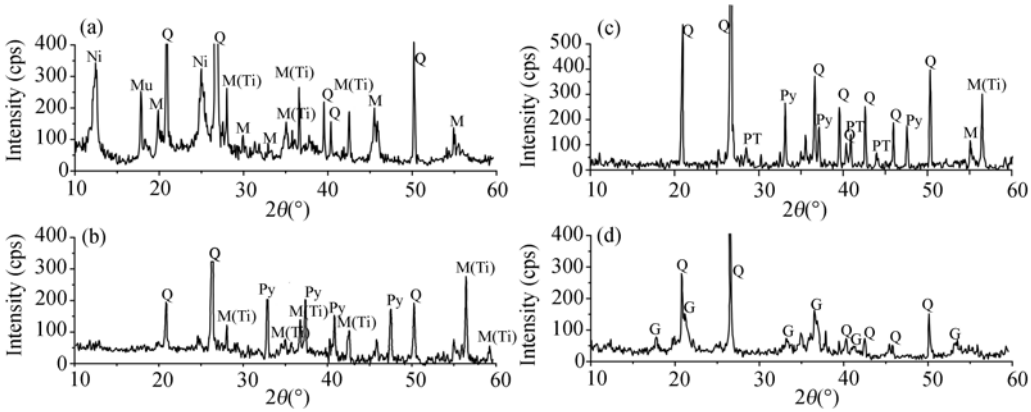

Figure 2 X-ray powder diffraction pattern for sediment samples after magnetic (a), (b), (d) or heavy liquid (c) extraction from PD core. (a), (b) First type sediment; (c) second type sediment; (d) third type sediment. Identified peaks are labeled for magnetite (M), titanomagnetite (M(Ti)), pyrite (Py), pyrrhotite (Pt), goethite (G), quartz (Q), nimite (Ni) and muscovite (Mu).

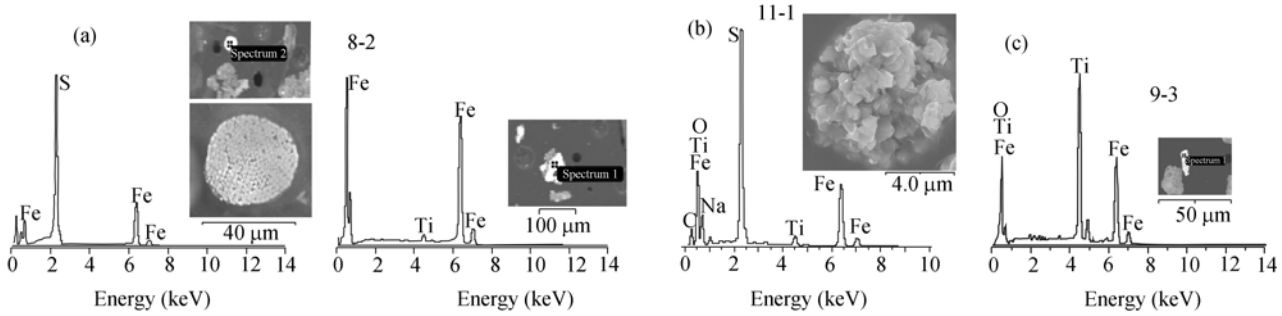

Figure 3 SEM image and energy dispersive spectra (EDS) for sediments of PD core. (a) First type sediment; (b) second type sediment; (c) third type sediment.

and inflexion in susceptibility at 580℃, but not tending towards zero until 680℃ (Figure 4(a))[12,13]. Cooling curves show a large increase of susceptibility at ~580℃, indicating the formation of additional magnetite during heating[12]. The marked increase of susceptibility at ~280℃ or ~350℃ may result from the decomposition of Fe-sulphides and the formation of more ferromagnetic minerals under argon atmosphere conditions[14,15]. Additional formation of ferromagnetic particles may also have occurred at temperature >500℃ from Fe-containing silicate/clay minerals or pyrite[12,13]. Combination of these possibilities causes the formation of a wide susceptibility peak.

Sediment samples of the second type are characterised by slowly decreasing susceptibility at temperatures <280℃, which may be ascribed to the gradual unblock-

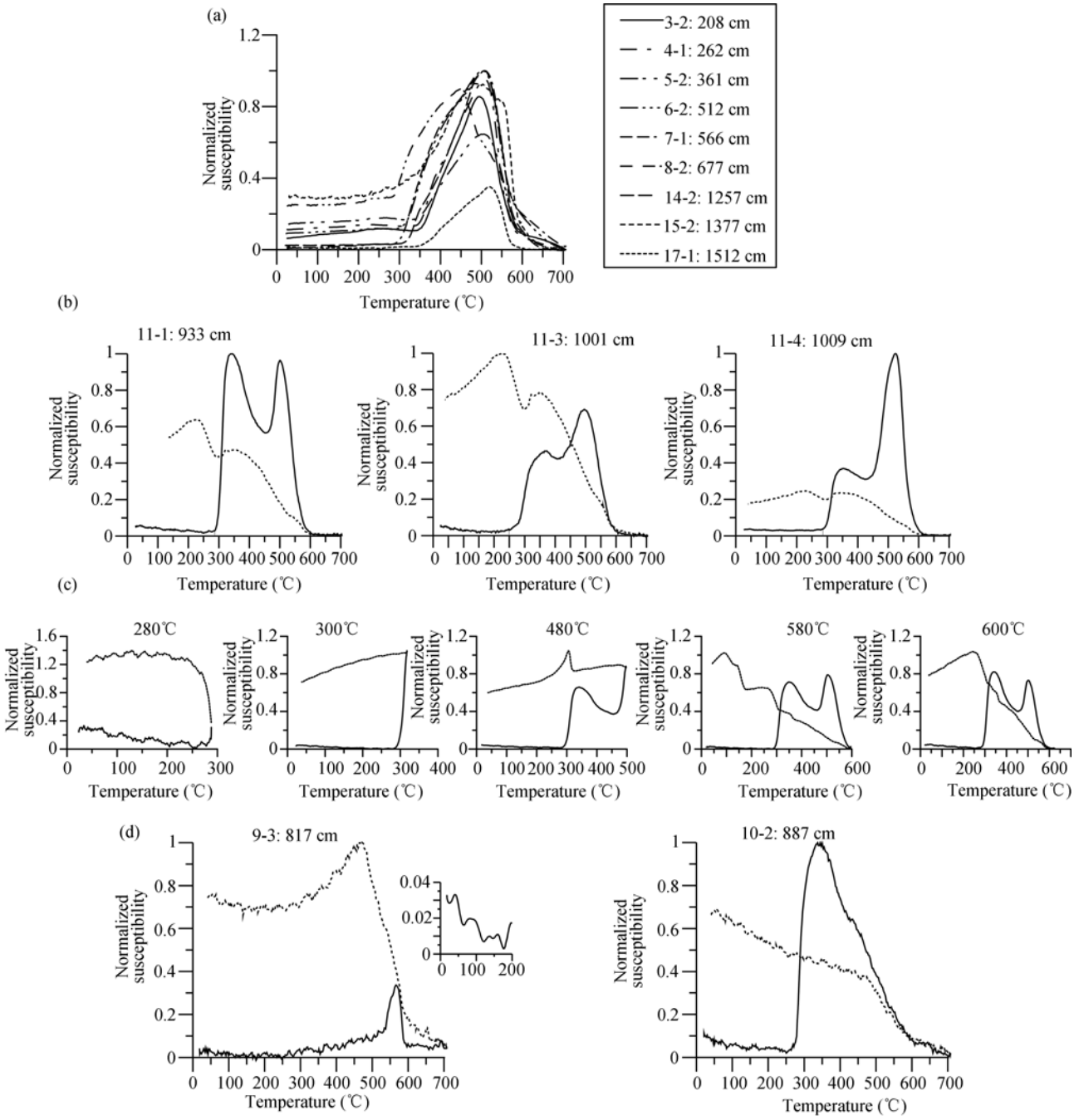

Figure 4 Temperature-dependent magnetic susceptibility curves for different types of sediments of PD core. Solid (dotted) lines represent heating (cooling) curves. (a) First type sediment; (b) second type sediment; (c) different maximum temperatures for second type sediment; (d) third type sediment.

ing of some fine magnetic particles (Figure 4(b))[6]. The χ-T curves show a double peak at temperature >280℃. Susceptibility begins to increase markedly at ~280℃ and reaches the first peak at ~350℃ followed by a decrease until another increase at 450℃. Susceptibility reaches the second peak at ~500℃ and then drops to near the initial value. Minimum susceptibility occurs at temperature >600℃ (Figure 4(b)). For different samples, the height of the first peak drops with decreases of H_{cr} and increases of the silt fraction. Stepwise temperature-dependent susceptibility curves show the formation of a great amount of ferromagnetic minerals at 280℃ (Figure 4(c)). The formation of pyrrhotite is indicated by an increase of susceptibility at 320℃ on the cooling curve while heating to 480℃[16]. The cooling curves reflect the unblocking temperature of fine-grained ferromagnetic minerals formed during heating to temperatures >580℃. With cooling to <580℃, susceptibility values are much lower than those of the heating curve at this temperature, indicating that magnetite is oxidized to hematite at temperature >580℃[12,16]. Hence, the first peak on the heating curve is due to the formation of Fe-sulphides and magnetite from Fe-containing paramagnetic minerals caused by burning of organic matter. The susceptibility of Fe-sulphides decreases within the range of its Curie temperature, with magnetite forming while heating to >450℃[14,15].

Some samples from the third type ("Huaban clay") of sediment are characterised by the susceptibility reaching a minimum while heating to 150℃ (Figure 4(d)). This suggests that the majority of magnetic minerals may be goethite (αFeOOH)[16,17]. An increase of susceptibility at temperatures >280℃ may be due to transformation of lepidocrocite (γFeOOH) to magnetic maghemite through dehydration[17]. The maximum peak of susceptibility is at ~516℃ followed by a drop to a minimum at ~585℃ that is mainly caused by the formation of magnetite from Fe-bearing silicates or clays[12,13]. The formation of hematite and magnetite during heating can be validated by the susceptibility during cooling being higher than during heating, slowly increasing at temperature directly below 700℃, but more rapidly while cooling to ~585℃. Other samples from the "Huaban clay" horizons show a rapid increase in susceptibility at ~260℃ and a pronounced peak at ~350℃, followed by a gradual decrease to a minimum at 700℃. This pattern indicates the dehydration of lepidocrocite to maghemite and a subsequent conversion of maghemite to hematite during the heating experiments[16].

4.3 Thermal demagnetization experiments of composite 3-axis IRM

Similar results to those described above can be achieved by Lowrie experiments carried out on sister samples [17]. For sediments of the first type, most of IRM resides in the low coercivity (<0.05 T) and medium coercivity (0.05—0.5 T) fractions (Figure 5(a)). A marked decay of remanence in the "soft" and "medium" magnetic fractions at around 250—300℃ suggests the presence of Fe-sulphides or titanomagnetite[17—20]. The remanence carried by the "soft" fraction declines to zero at 580℃, which indicates the unblocking temperature of magnetite[16,17]. The unblocking temperature of hematite is shown by the remanence minimum of the "medium" and "hard" fractions at 650℃[16,17].

For sediments of the second type, the remanence of the "medium" and "hard" fractions notably increases, and the shapes of thermal demagnetization curves for IRM change with H_{cr} (Figure 5(b)). For grey-black clay samples with very low remanence, the components carried by the "soft" and "medium" fractions show a slight decrease at 550℃, and run to near zero at 650℃ (sample 11-1). For silty clay samples, the remanent intensity is higher than for the grey-black clay samples, and the contribution to remanence of the "soft" fraction increases and is associated with an inflection of intensity of the "soft" and "medium" fractions at ~250—~300℃. A clear decay of the "soft" fraction remanence occurs similarly between 500—580℃. The remanence of all fractions reaches zero at ~650℃ (11-4). The decay of remanence at 550℃, 500—580℃ should be caused by the thermal properties of magnetite, and that between 250—300℃ by Fe-sulphides[18,20]. These results show the occurrence of magnetite, Fe-sulphide and hematite in this type of sediments[17,18,20,21], but the fraction of magnetite and hematite is so small that their contribution to remanence is negligible. They also indicate an increase of Fe-sulphides with medium coercive force which contribute more to remanence.

For the third type "Huaban clay" samples, the remanence for some samples is mainly dominated by the "hard" and "medium" fractions that decrease to zero at

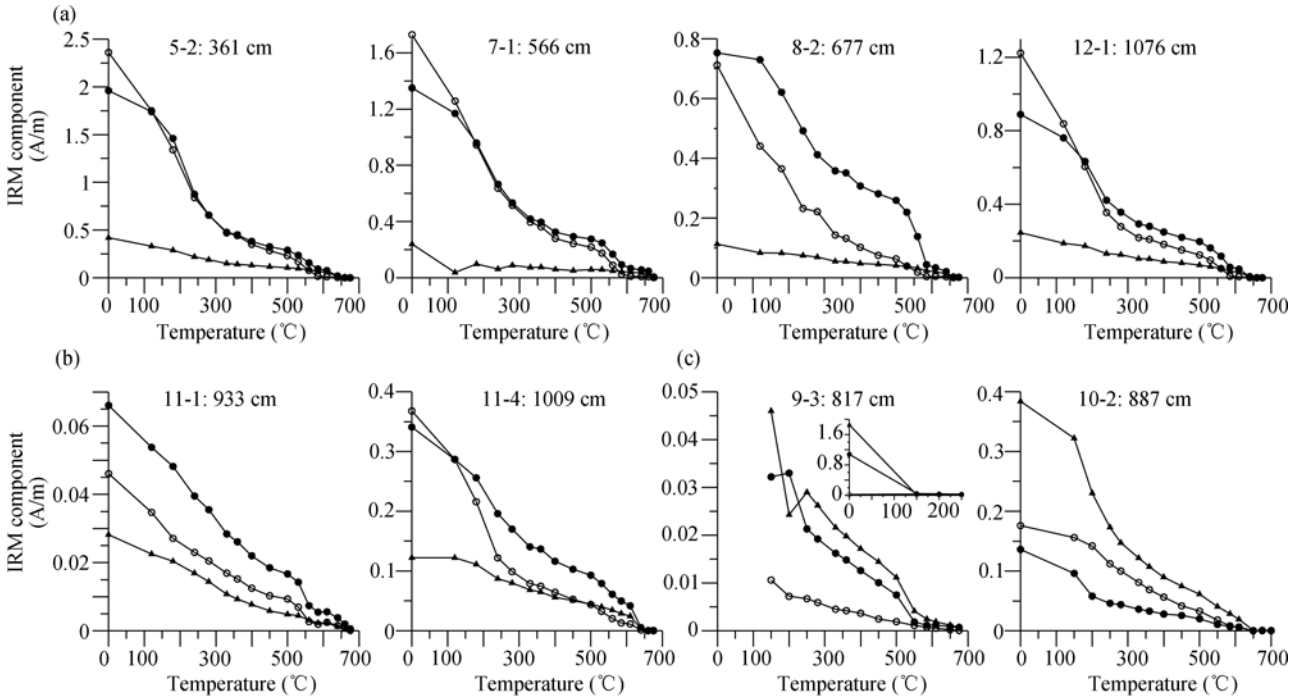

Figure 5 Thermal demagnetization of three component IRM of PD core sediments. Hollow circle, soft fraction; solid circle, medium fraction; triangle, hard fraction. (a) First type sediment; (b) second type sediment; (c) third type sediment.

150℃ (sample 9-3). This is typical of goethite[16] (Figure 5(c)). However, remanent variations carried by the "soft" and "medium" fractions at 550℃ indicate the presence of some magnetite as well[16]. For the "hard" and "medium" fractions of other samples, the remanence reaches zero at ~650℃ (sample 10-2), indicating the presence of hematite[16,17].

4.4 Acquisition curves of IRM and H_{cr} spectra

Features of acquisition curves of IRM and H_{cr} spectra for 20 samples from different layers are consistent with the results mentioned above (Figure 6). For sediments of the first type, IRM increases sharply in initial low fields and reaches SIRM at 1000 mT. The remanent coercivities for all samples range between 30—50 mT (Figure 6(a)). These properties suggest that sediment remanence is mainly carried by low coercivity magnetic minerals[16,17,22], i.e. mainly magnetite.

For sediments of the second type, IRM reashes 50%—65% of SIRM at 100 mT and 70%—80% at 300 mT. H_{cr} varies between 48—110 mT with grain size of the sediments (Figure 6(b)), with its lower values corresponding to coarser sediments (e.g. silty clay). These suggest that medium coercivity minerals are presented in this type of sediments[19,21,23—25], and should mainly be Fe-sulphides as indicated by XRD, EDS and χ-T.

The SIRM and H_{cr} curves for the third type of sediments ("Huaban clay") have two patterns. One has IRM tending towards saturation at 2700 mT, but the IRM increases slowly while the field is less than 1000 mT. H_{cr} falls between 170—240 mT (Figure 6(c)). These features indicate that magnetic minerals, i.e. mainly hematite, dominate the remanence[16,17,25]. The other has very high H_{cr} (~630 mT). The IRM increases very slowly and does not reach SIRM even at 2700 mT. These indicate the predominance of goethite in magnetic minerals[16,25].

4.5 Hysteresis loop parameters

It was noted that paramagnetic minerals have a significant impact on the hysteresis loop parameters of all samples, varying considerably in accordance with the sediment type (Figure 7(a)). Magnetization of the first type sediments increases linearly with magnetic field when the latter is higher than 300 mT. When magnetic field is below 300 mT, however, the overall curve displays an 'S' shape. Hysteresis loop parameters of the second type sediments are largely determined by the paramagnetic minerals so that the curve is close to a straight line. As for the third type sediment, the curve is linear when the magnetic field is >300 mT and wide when <300 mT.

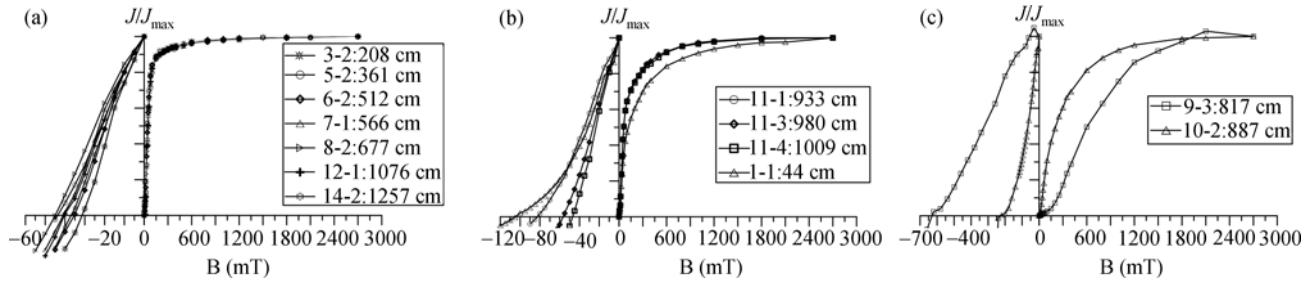

Figure 6 SIRM acquisition, back field curves of some PD core sediment samples. (a) First type sediment; (b) second type sediment; (c) third type sediment.

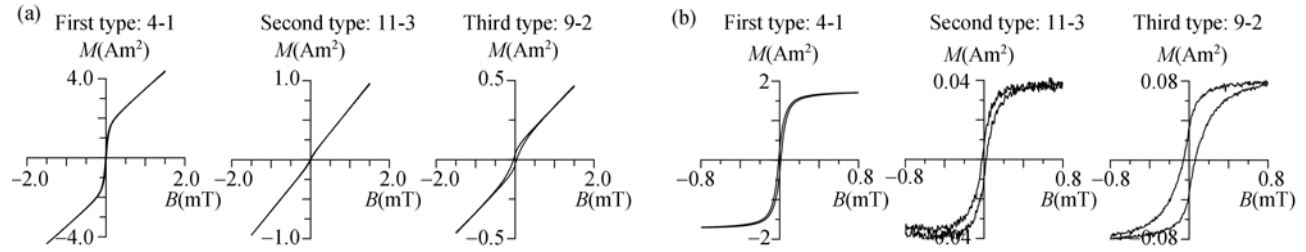

Figure 7 Comparison of hysteresis loops for the different type PD core sediments (field unit: $\times 10^3$ mT, intensity unit: $10^{-4}Am^2$). (a) Including paramagnetism; (b) removal of paramagnetism.

After removal of paramagnetic mineral signal (Figure 7(b)), the hysteresis loop of the first type sediment shows a tendency to close in the magnetic field of approximately ±500 mT, with M_{rs}/M_r between 0.11 and 0.17 and H_{cr}/H_c between 2.35 and 3.3, suggesting that this type of magnetism is predominantly determined by titanomagnetite of low coercivity in the PSD state[13,25,26]. The hysteresis loops of the second and third types of sediments have a "wasp-waisted" shape rather than a closure. The curves derived from SIRM and the respective IRM thermal demagnetization curves indicate high coercive force components in the two types of sediments. The "wasp-waisted" curve shape is due to the co-presence of both high and low coercive force magnetic components. In the second type sediment, M_{rs}/M_s is ~ 0.22 and H_{cr}/H_c ~4.1. These data differ significantly from those reported for greigite, probably representing pyrrhotite. The M_{rs}/M_s ratio of 0.43 and H_{cr}/H_c of 2.8 imply the occurrence of hematite in third type sediment.

5 Discussion

5.1 Magnetic mineral types of sediment

Based on the results described above, the magnetic minerals in the Pearl River Delta sediments can be grouped into three different types. The first type has magnetite or titanomagnetite as the primary magnetic minerals, with accessory hematite and minor Fe-sulphides. It is associated with sediments dominating the core. Fe-sulphides should have a limited impact on the magnetic properties of the sediments.

The second type contains a large quantity of paramagnetic minerals, but with a small amount of Fe- sulphides as the dominant magnetic phase. It corresponds to sediments occurring within the top 44 cm and between ~913—~1010 cm in the middle part of the core where the grain size is the smallest and the magnetic susceptibility is the lowest (with even negative values and an average of -0.19×10^{-5} SI) in the whole core. The absence of fossil such as foraminifera and ostracod in the two periods of sediments indicates a swampy environment possibly resulting from a regression.

The dominant magnetic minerals in the third type are hematite and goethite produced during weathering process under hot-humid climate, suggesting a period of exposure and no sedimentation.

5.2 Environmental implications

(i) Variations of coercivity and sea-level fluctuation. The *S*-ratio value varies considerably for the three types of sediment (Figure 8). For the first type sediments, the S_{100} ratio (IRM_{100mT}/IRM_{1000mT}) is usually >0.8 and S_{300} ($IRM_{-300mT}/IRM_{1000mT}$) close to ~0.9. The S_{100} and S_{300} values for the second type of sediments are ~0.55 respectively, while for the third type, ~0.3. These magnetic characteristics indicate that magnetic properties of

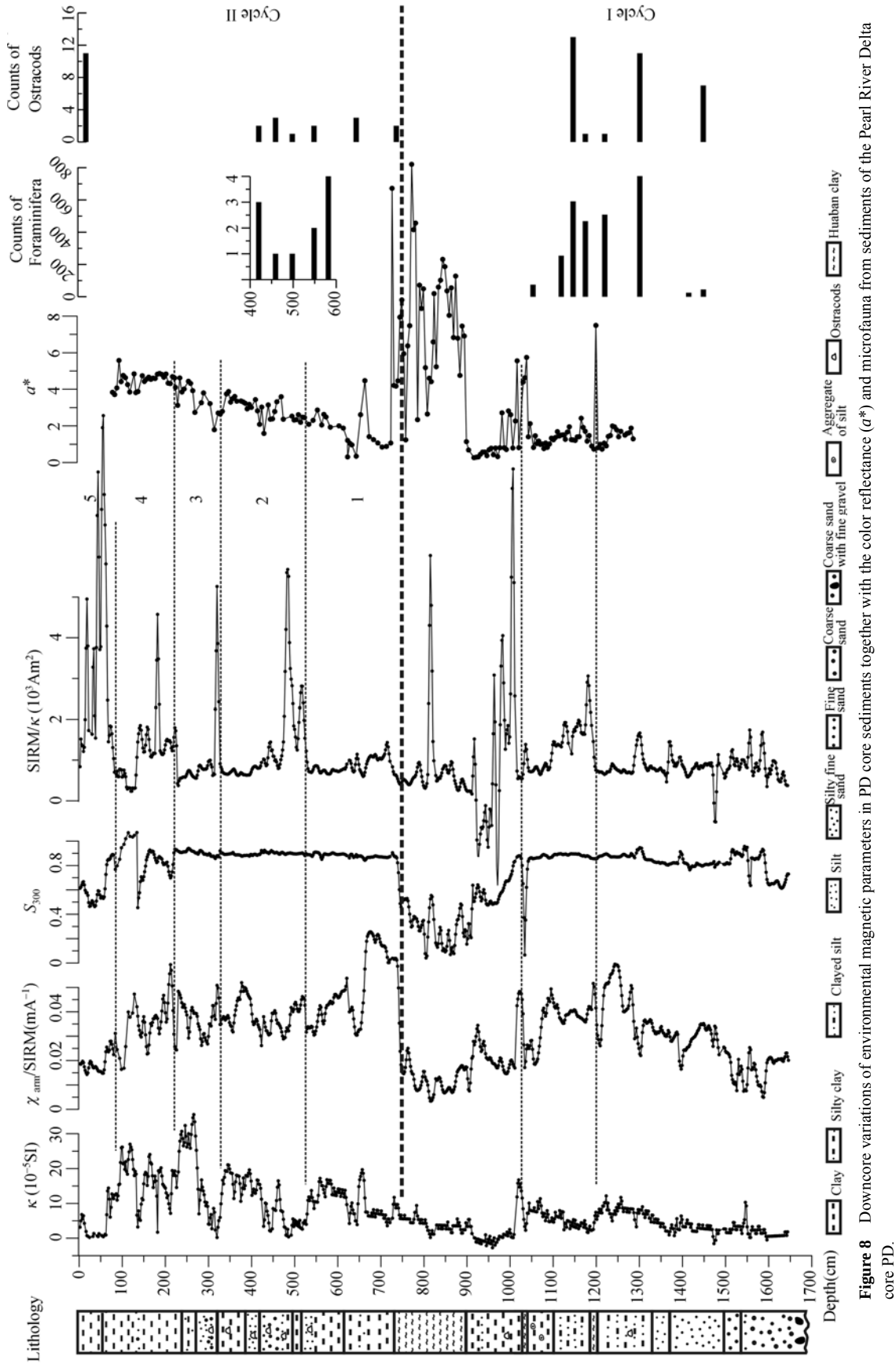

Figure 8 Downcore variations of environmental magnetic parameters in PD core sediments together with the color reflectance (a^*) and microfauna from sediments of the Pearl River Delta core PD.

naturally deposited sediments are controlled by detrital magnetite[6,27−30], of which the concentration and grain size should be controlled by estuarial hydrodynamics. Increasing H_{cr} and changes in the type of magnetic minerals indicate significant changes in sedimentary environment. Fe-sulphides with high coercivity dominate the magnetic properties of sediments consisted of grey-black clay (with a minimum redness a^* value of color reflectance), in which concentrations of C and N are high and foraminifera and ostracoda are absent, suggesting an anoxic swamp environment[30]. Goethite and hematite dominate the magnetic properties and H_{cr} displays a maximum in the "Huaban clay" (with a maximum a^* value of the color reflectance), indicating a marine regression, exposure of sediments to a humid environment and oxidation. Thus, a change of coercivity from low to high can be correlated with a marine regression.

(ii) Grain size of magnetic minerals and sea-level fluctuation. The linear correlation between volume susceptibility (κ) and SIRM for the first type of sediment shows that variations of κ and SIRM mostly arise from the concentration of magnetite (Figure 9(a)). Some points deviating from the trend line of the SIRM-κ plot with higher SIRM/κ ratios reflect increases of fine magnetic mineral fraction[6,29,31], which may be related with a reduced hydrodynamics with increasing water depth. The notable high value of SIRM/κ coincides with the grey-black clay which coarsens upwards, and the presence of foraminifera. Thus, fluctuations of SIRM/κ ratio of this type of sediments may reflect cycles of marine transgression and regression. The deviation of some points from the SIRM-κ trend line with relatively high SIRM/κ ratios, which correspond to sediments at intervals of 913−1010 cm and 0−44 cm in the core, reflects a swampy environment associated with the gradual change in type and grain size of magnetic minerals[6,29,31]. The samples from the "Huaban clay" are also scattered on the SIRM-κ plot, but distributed above the trend line with relatively lower SIRM/κ ratios. This should be caused by changes in the concentration of high coercivity minerals such as goethite.

Although there is somewhat scattering on the plot of χ_{arm}/SIRM versus κ, a positive correlation could be observed between χ_{arm}/SIRM and κ (Figure 9(b)), indicating that fining of grain size is accompanied by increasing in concentration of magnetic minerals[29,31]. The χ_{arm}/SIRM ratio is independent of S_{300} for the first type sediment (Figure 9(c)), further confirming the influence of grain size of magnetic mineral on magnetic parameters. χ_{arm}/SIRM varies with a higher frequency than SIRM/κ along the core, but their overall trends are similar (Figure 8). The fining of grain size coupled with an increasing of magnetic mineral fraction may point to a marine transgression. Therefore parameters of SIRM/κ and χ_{arm}/SIRM, which reflect variation of fine magnetic mineral fraction, can be used as proxies for sea-level fluctuation.

According to downcore variations of environmental magnetic parameters and sedimentary characteristics, the environmental evolution recorded by the PD core can be divided into two main cycles (Figure 8). Cycle I (1650−740 cm) terminates at the top of the "Huaban clay" at a depth of 7.4 m. During this cycle, susceptibility and χ_{arm}/SIRM vary from low to high and then back to low, and concentration of microfauna shows a similar trend as well, suggesting a complete cycle from marine transgression to regression. During Cycle II (740−0 cm), a similar variation of susceptibility, χ_{arm}/SIRM, microfauna and inferred sea level change to Cycle I is observed except that the frequency of these features is

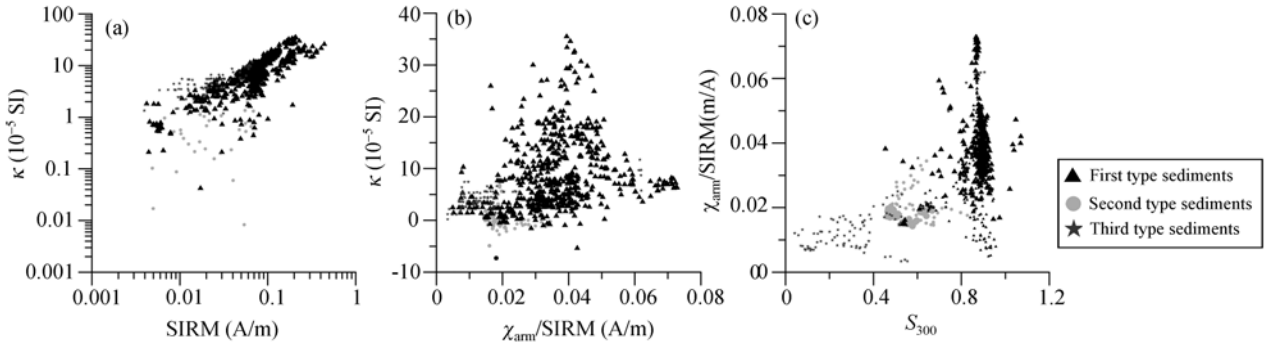

Figure 9 Biplots of multi-parameters of environmental magnetic indicators in PD core.

higher. Three sub-cycles of sea-level fluctuation can be identified in cycle I according to the variations of χ_{arm}/SIRM and SIRM/κ as well as the two thin but notable marker layers of "Huaban clay". During Cycle II, five sub-cycles of sea-level fluctuation are suggested according to the variations of SIRM/κ and χ_{arm}/SIRM. The original sediments for the "Huaban clay" are altered by strong weathering. Thus the magnetic proxies of SIRM/κ and χ_{arm}/SIRM for the "Huaban clay" reflect the weathering process rather than sea-level fluctuation.

According to age determination by ^{14}C and TL dating methods and correlation with an adjacent core [32], Cycle I is estimated to be in the Late Pleistocene and Cycle II in the Holocene with a sedimentation hiatus in between. Thus, PD core suggests that there are two significant marine transgressions in the Pearl River Delta since the Late Pleistocene. This is consistent with previous investigations carried out in this area[33]. The two transgressions may have experienced sea-level change with similar amplitude, but the one during the Holocene with more frequent fluctuations relative to the other during the late Pleistocene. At least a total of eight sub-cycles of sea-level fluctuation have occurred since deposition of the Pearl River Delta sediments began.

6 Conclusions

(1) The magnetic mineral assemblage of sediments from core PD can be divided into three types. In the first type, magnetic properties are mainly dominated by magnetite, with minor hematite and Fe-sulphides having little effect on magnetic properties. In the second type, the main magnetic mineral is Fe-sulphides together with a very low fraction and amounts of paramagnetic minerals. In the third type ("Huaban clay"), hematite and goethite are the dominant magnetic minerals.

(2) The different assemblages of magnetic minerals indicate different sedimentary environments. Magnetite with low H_{cr} occurs in sediments deposited during sea level fluctuation with small amplitude. Increasing H_{cr} indicates a swampy environment following marine regression where Fe-sulphides are dominant. Hematite and goethite with very high H_{cr} suggest strong chemical weathering under hot-humid climate.

(3) Variations of the concentration and grain size of magnetic minerals indicate changes in hydrodynamic conditions whereas the magnetic properties of sediments are dominated by low coercivity minerals. The magnetic parameters of SIRM/κ and χ_{arm}/SIRM that indicate the fraction of fine-grained magnetic minerals may be used as proxies for sea-level fluctuation with their higher values corresponding to more fraction of fine-grained magnetic minerals and reflecting increasing sea-level.

(4) Sediments in the PD core indicate two major sedimentary cycles related to marine transgression and regression during the Late Pleistocene and Holocene. The cycle in the Late Pleistocene includes three sub-cycles and the one in the Holocene, five sub-cycles.

We are grateful to Dr. Yang Shiling, who measured sediment color reflectance, and Drs. Deng Chenglong, Li Haiyan, and Dong Yixin for helpful discussions during preparation of the paper.

1 Tamura T, Saito Y, Sieng S, et al. Depositional facies and radiocarbon ages of a drill core from the Mekong River lowland near Phnom Penh, Cambodia: Evidence for tidal sedimentation at the time of Holocene maximum Xooding. J Asian Earth Sci, 2007, 9: 585－592[DOI]
2 Hori K, Tanabe S, Saito Y, et al. Delta initiation and Holocene sea-level change: example from the Song Hong (Red River) delta, Vietnam. Sediment Geol, 2004, 164: 237－249[DOI]
3 García-García F, Fernández J, Viseras C, et al. High frequency cyclicity in a vertical alternation of Gilbert-type deltas and carbonate bioconstructions in the late Tortonian, Tabernas Basin, Southern Spain. Sediment Geol, 2006, 192: 123－139[DOI]
4 Goodbred S L. Response of the Ganges dispersal system to climate change: a source-to-sink view since the last interstade. Sediment Geol, 2003, 162(1-2): 83－104[DOI]
5 Heroy D C, Kuehl S A, Goodbred S L. Mineralogy of the Ganges and Brahmaputra Rivers: implications for river switching and Late Quaternary climate change. Sediment Geol, 2003, 155(3-4): 343－359[DOI]
6 Thompson R, Oldfield F. Environmental Magnetism. London: Allen & Unwin Ltd., 1986
7 Liu Q S, Deng C L, Torrent J, et al. Reviews on recent developments of mineral magnetism of the Chinese loess. Quat Sci Rev, 2007, 26: 368－385[DOI]
8 Verosub K L, Roberts A P. Environmental magnetism: past, present, and future. J Geophys Res, 1995, 100: 2175－2192[DOI]
9 Deng C L, Liu Q S, Pan Y X. Environmental magnetism of Chinese loess/plaeosol sequences. Quat Sci (in Chinese), 2007, 27(2): 193－209
10 Huang Z G, Li P R, Zhang Z Y, et al. Formation, Development and Evolution of the Zhujiang Delta (in Chinese). Guangzhou: Science and Technology Press of Guangzhou, 1982
11 Long Y Z, Huo C L. The sedimentation characteristics of Zhujiang River Delta in late Quaternary. Mar Sci (in Chinese), 1990, 4: 7－14
12 Deng C L, Zhu R X, Jackson M J, et al. Variability of the temperature-dependent susceptibility of the Holocene Eolian deposits in the Chinese Loess Plateau: a pedogenesis indicator. Phys Chem Earth (A),

2001, 26(11-12): 873－878[DOI]
13 Deng C L, Zhu R X, Kenneth L et al. Mineral magnetic properties of loess/paleosol couplets of the central Loess Plateau of China over the last 1.2 Ma. J Geophys Res, 2004, 109: B01103[DOI]
14 Andrew P R. Magnetic properties of sedimentary greigite (Fe_3S_4). Earth Planet Sci Lett, 1995, 134: 227－236[DOI]
15 Chorng-Shern H, Andrew P R. Authigenic or detrital origin of pyrrhotite in sediments: resolving a paleomagnetic conundrum. Earth Planet Sci Lett, 2006, 241: 750－762[DOI]
16 Dunlop D J, Ozden O. Rock Magnetism. Cambridge: Cambridge University Press, 1997
17 Lowrie W. Identification of ferromagnetic minerals in rock by coercivity and unblocking temperature properties. Geophys Res Lett, 1990, 17(2): 159－162
18 Sagnotti L, Winkler A. Rock magnetism and paleomagnetism of greigite-bearing mudstones in the Italian peninsula. Earth Planet Sci Lett, 1999, 165: 67－80[DOI]
19 Menyeh A, Reilly W O. The coercive force of fine particles of monoclinic pyrrhotite (Fe_7S_8) studied at elevated temperature. Phys Earth Planet Inter, 1995, 89: 51－62[DOI]
20 Hu S Y, Appel E, Hoffmann V, et al. Identification of greigite in lake sediments and its magnetic significance. Sci China Ser D-Earth Sci, 2002, 45(1): 81－87
21 Shi C D, Zhu R X. Identification and origins of iron sulfides in Czech loess. Geophys Res Lett, 2001, 28(20): 3903－3906[DOI]
22 Vigliotti L. Magnetic properties of light and dark sediment layers from the Japan Sea: diagenetic and paleoclimatic implications. Quat Sci Rev, 1997, 16: 1093－1114[DOI]
23 Emiroglu S, Rey D, Petersen N. Magnetic properties of sediment in the Ria de Arousa (Spain): dissolution of iron oxides and formation of iron sulphides. Phys Chem Earth, 2004, 29: 947－959
24 Ishikawa N, Frost G M. Magnetic properties of sediments from Ocean Drilling Program sites 1109, 1115, and 1118 (Leg 180), Woodlark Basin (Papua New Guinea). Earth Planets Space, 2002, 54: 883－897
25 Peters C, Thompson R. Magnetic identification of selected natural iron oxides and sulphides. J Mag Mag Mater, 1998, 183: 365－374[DOI]
26 Roberts A P, Cui Y, Verosub K L. Wasp-waisted hysteresis loops: Mineral magnetic characteristics and discrimination of components in mixed magnetic systems. J Geophys Res, 1995, 100, B9: 17909－17924[DOI]
27 Liu J, Zhu R X, Li S Q, et al. Magnetic mineral diagenesis in the post-glacial muddy sediments from the southeastern South Yellow Sea: Response to marine environmental changes. Sci China Ser D-Earth Sci, 2005, 48(l): 134－144
28 Liu J, Zhu R X, Roberts A P, et al. High-resolution analysis of early diagenetic effects on magnetic minerals in post-middle-Holocene continental shelf sediments from the Korea Strait. J Geophys Res, 2004, 109: B03103[DOI]
29 Beatriz O, Cecilia C, Socorro L, et al. 52000 years of environmental history in Zacapu basin, Michoacan, Mexico: the magnetic record. Earth Planet Sci Lett, 2002, 202: 663－675[DOI]
30 Gao F L, Yang X Q, Dong Y X, et al. Carbon-Nitrogen record in sediments of core PD in the Pearl River Delta and the environmental significance. Mar Geol Quat Geol (in Chinese), 2006, 26(2): 33－39
31 Moreno E, Thouveny N, Delanghe D, et al. Climatic and oceanographic changes in the Northeast Atlantic reflected by magnetic properties of sediments deposited on the Portuguese Margin during the last 340 ka. Earth Planet Sci Lett, 2002, 202: 465－4800[DO]
32 Zhang W Q, Huang Z G. The cooling fluctuation events during Holocene in the tropical zone of China. Trop Geogr (in Chinese), 2005, 125(14): 298－321
33 Chen M H, Zhao H T, Wen X S. Quaternary foraminiferal group and sporopollen zones in cores L2 and L16 in the Lingdingyang Estuary. Mar. Geol Quat Geol (in Chinese), 1994, 14(1): 11－22